ARTICLE

"Giant" Hollow Multilayer Capsules by Microfluidic Templating

M. Talha Gokmen,[†] Bruno G. De Geest,[†,§] Wim E. Hennink,[†] and Filip E. Du Prez*[,†]

Polymer Chemistry Research Group, Department of Organic Chemistry, and Department of Pharmaceutics, Ghent University, 9000 Ghent, Belgium, and Department of Pharmaceutics, Utrecht University, 3584 CA Utrecht, The Netherlands

ABSTRACT Monodisperse microgels were synthesized by a microfluidic setup and used as a sacrificial template for the fabrication of "giant" hollow polyelectrolyte capsules with rigid walls consisting of covalently cross-linked polyelectrolytes and metal nanoparticles. First, a simple tubing−needle-based microfluidic system is utilized to produce size-monodisperse, degradable "giant" microgels consisting of dextran chains linked via carbonate esters. Second, these monodisperse microgels are subjected to a layer-by-layer coating of negatively charged platinum nanoparticles (Pt_{NP}'s) and a positively charged diazoresin (DAR). Three bilayers of Pt_{NP}'s and DAR are used to obtain a stable membrane on the microgels. Finally, the sacrificial dextran-based microgel cores are smoothly hydrolyzed and removed without rupture of the polyelectrolyte membrane due to the covalently linked hybrid polyelectrolyte/nanoparticle nature of the membrane. Scanning electron and confocal microscopy are used to characterize the capsules. The capability of encapsulating materials of interest is also shown by the addition of fluorescent polystyrene particles to the monomer mixture and subsequent visualization of embedded polystyrene particles in coated microgels after microfluidic polymerization and layer-by-layer coating. The obtained "giant" microcapsules are envisaged to be used as microreactors or drug-delivery systems.

KEYWORDS: polyelectrolyte • layer-by-layer • capsule • microfluidics • monodisperse • nanoparticle

INTRODUCTION

Polyelectrolyte microcapsules have attracted increased attention for different purposes such as for delivery and as biosensors and microreactors. These microcapsules are usually fabricated by alternate layer-by-layer (1−4) deposition of charged species onto an oppositely charged template followed by decomposition of this template (5−14). Both hydrogels (15−17) and emulsions (18−21) have recently gathered increased interest to serve as such sacrificial templates in which the species of interest are being encapsulated within the template during their synthesis. This method benefits from the easy encapsulation procedure and mild conditions required to remove the template after polyelectrolyte coating. An inherent feature of emulsions is the polydispersity of their size distribution. However, production of monodisperse emulsions would offer considerable benefits such as equal distribution of the encapsulated material over different droplets and a better prediction and control of the behavior of the entire population.

Since the advent of microfluidic emulsification (22), several papers have been reported on the fabrication of particulate material in microfluidic devices (23−26). Among the many types of hydrophobic particles, also hydrophilic microgels based on alginic acid cross-linked by microfluidic mixing with calcium ions (27) as well as methacrylate dextran microgels cross-linked by UV-initiated radical polymerization have been reported (28). The latter research, reported by De Geest et al., described the synthesis of 10-μm-sized, degradable hydroxyethyl methacrylate−dextran (dex-HEMA (29, 30); see the structure in Figure 1A) microgels in poly(dimethylsiloxane)-based microfluidic chips. Moreover, there is a recent report on the synthesis of microcapsules via a layer-by-layer deposition technique in microfluidic chips (31).

In this research, we aimed at fabricating hollow polyelectrolyte capsules using monodisperse dex-HEMA microgels as sacrificial templates, which were obtained by a simple microfluidic setup. A special feature added to this aim is the size of the microcapsules. While polyelectrolyte microcapsules are traditionally fabricated on microparticles such as polystyrene, melamine formaldehyde, silica or inorganic carbonate with dimensions varying from 1 to 10 μm (9), we aim to produce stable, "giant" capsules with sizes of several hundreds of micrometers. Such microcapsules could find application as, e.g., microreactors because their size would allow higher production capacities while still having the benefits of a confined geometry (32−34).

When we initiated the research on polyelectrolyte-coated microgels, the purpose was to develop self-exploding microcapsules. As reported in several of our papers, such microcapsules consist of a degradable dex-HEMA microgel core surrounded by a polyelectrolyte membrane (16, 35). Upon microgel core degradation, the swelling pressure increases, and at a certain moment, when the swelling pressure exceeds the membrane's tensile strength, the capsule explodes and releases its contents. In this concept, two parameters play a prominent role: the tensile strength

* Tel: +32 9 264 45 03. Fax: +32 9 264 49 72. E-mail: filip.duprez@ugent.be.
Received for review January 27, 2009 and accepted May 5, 2009
[†] Department of Organic Chemistry, Ghent University.
[‡] Utrecht University.
[§] Department of Pharmaceutics, Ghent University.
DOI: 10.1021/am900055b

Published on Web 05/21/2009

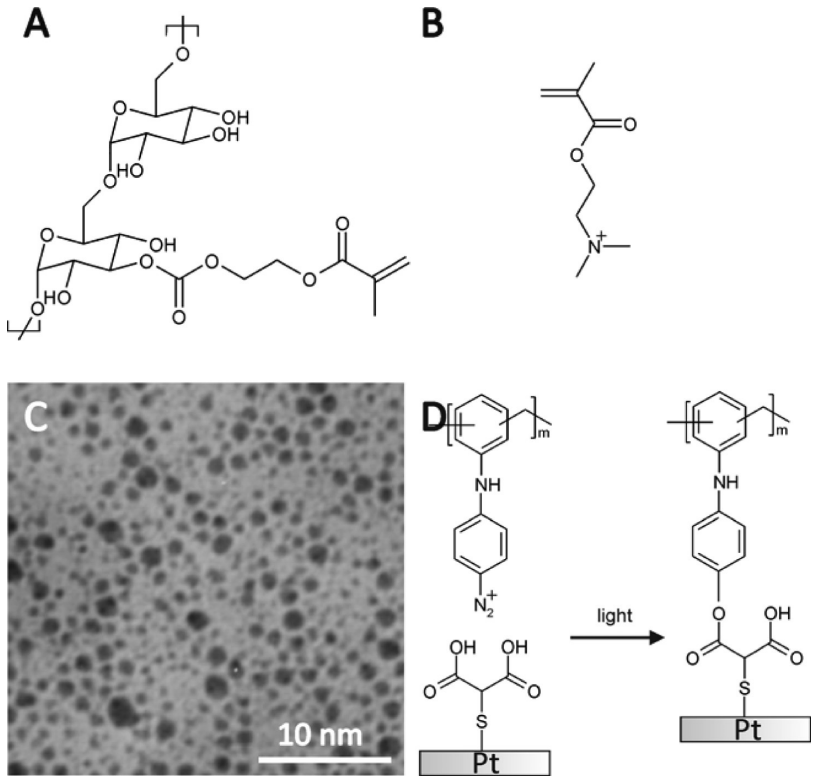

FIGURE 1. Molecular structures of (A) dex-HEMA and (B) DMAEMA (positively charged). (C) TEM image of the Pt_{NP}'s used for the multilayer buildup. (D) Molecular structure of the light-induced covalent reaction between the diazo moieties of the DAR and the carboxylic acid moieties on the surface of the Pt_{NP}'s.

of the membrane and the swelling pressure of the microgels. Moreover, Laplace's law predicts that larger microgels will require less pressure than smaller microgels to rupture a membrane with the same thickness. Taking these considerations into account, we were able to develop a variety of exploding microcapsules by varying the membrane composition and microgel size (16, 35−39). However, because we aimed for stable polyelectrolyte capsules in this project, i.e., avoiding the self-exploding property, some fine-tuning has been required on two levels. First, we lowered the swelling pressure of the degrading microgels by decreasing the solid content of the microgels from 30 to 17 wt %. Second, we attempted to strengthen the capsules' membrane by employing a so-called "hybrid" polyelectrolyte/nanoparticle coating comprising alternating layers of negatively charged platinum nanoparticles (Pt_{NP}'s) and a diazoresin (DAR), a cationic polyelectrolyte. Several groups have already reported on the enhanced mechanical properties of multilayer films containing nanoparticles (40, 41). Moreover, the DAR is able to form a covalent linkage with the carboxylic acid moieties present on the surface of the Pt_{NP}'s (42), which was expected to further increase the membrane's strength.

EXPERIMENTAL SECTION

Materials. (Dimethylamino)ethyl methacrylate (DMAEMA), hydrogen hexachloroplatinate hexahydrate ($H_2PtCl_6 \cdot 6H_2O$), mercaptosuccinic acid (MSA), sodium borohydride ($NaBH_4$), mineral oil, and suspensions of fluorescent polystyrene beads with diameters of both 100 nm and 1 μm were purchased from Sigma-Aldrich. Tygon tubing (0.8 mm internal diameter, Saint-Gobain Performance Plastics) were purchased from VWR International. 30G disposable needles were purchased from Becton Dickinson and blunted. A Metalight UV box operating with 12 (320−400 nm) lamps was used for solidification. Irgacure 2959 was obtained from Ciba. ABIL EM-90 was kindly donated by Evonik Degussa. The diazoresin (diazo-10, 4-diazodiphenylamine/formaldehyde condensate hydrogen sulfate/zinc chloride salt) was purchased from Livingston Associates, PC. Dex-HEMA was synthesized according to the literature (29).

Synthesis of Pt_{NP}'s. A total of 647 mg (1.25×10^{-3} mol) of $H_2PtCl_6 \cdot 6H_2O$ was dissolved in 5 mL of water. A total of 188 mg (1.25×10^{-3} mol) of MSA was dissolved in 245 mL of methanol. Both solutions were mixed and stirred for 30 min at room temperature. A total of 473 mg (12.5×10^{-3} mol) of $NaBH_4$ was dissolved in 25 mL of water and dropwise added to the $H_2PtCl_6 \cdot 6H_2O$/MSA mixture under vigorous stirring. During the addition of $NaBH_4$, the solution gradually turned dark and the Pt_{NP}'s formed as a dark precipitate. The reaction mixture was further stirred for 1 h at room temperature. Afterward the reaction mixture was centrifuged at 4000 rpm for 5 min and the supernatant was discarded. Three washing/centrifugation steps with methanol wewre performed, and finally the Pt_{NP}'s were dried under vacuum.

UV−Vis Monitoring of the Multilayer Buildup. Quartz slides were cleaned and hydrophilized by treatment with a freshly prepared piranha solution (35% H_2O_2/98% H_2SO_4 (1:1, v/v); ***Caution!*** *piranha solution reacts violently with organic materials and should not be stored in closed containers*) and then abundantly rinsed with distilled water. The treated quartz slides were precoated with a poly(etherimide) (PEI) layer by immersion in a 2 mg/mL PEI solution containing 0.5 M NaCl. Multilayers of Pt_{NP}/DAR were deposited on the PEI-coated quartz slides starting with the negatively charged Pt_{NP} by immersion in a 0.5 mg/mL Pt_{NP} solution (containing 0.5 M NaCl) for 10 min followed by rinsing with pure water. Finally, the quartz slides were dried under a nitrogen stream. Then the DAR layer was deposited

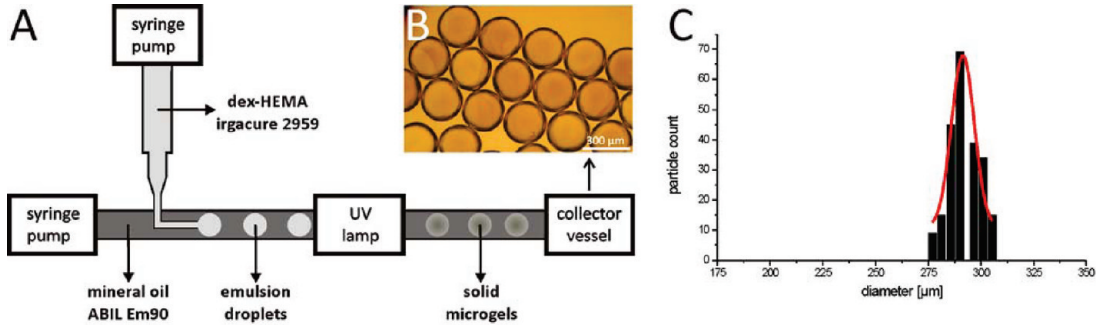

FIGURE 2. (A) Schematic representation of the tubing-based microfluidic setup. (B) Optical microscopy image of the obtained monodisperse microgels. (C) Size distribution histogram of the microgels, with the red curve representing a Gaussian fit ($n = 250$).

from a 2 mg/mL DAR solution (containing 0.5 M NaCl). This was repeated until the desired amount of bilayers was deposited. After each deposition of a layer, the absorbance of the film was measured with a Pharmacia Biochrom 4060 UV−vis spectrophotometer.

Microfluidic Emulsification. The pumping rates of continuous and discrete phases were 60 and 1 mL/h, respectively. A 2-m piece of Tygon tubing was used, which allowed the formed droplets to be exposed to UV light for approximately 45 s. The tubing makes few helices inside the chamber in which the UV lamps are distributed on the outer circle. This 45 s was enough to fix the structure of the beads, but complete conversion was ensured with 15 min of extra off-tubing UV exposure by simply leaving the collected beads in the UV chamber. The continuous phase was prepared by dissolving 4.5% (by volume) of ABIL EM-90 in mineral oil. The discrete phase was prepared by first dissolving 20 mg of Irgacure 2959 in 1 mL of distilled water, which was warmed up to 70−80 °C in a water bath. After cooling to room temperature, 200 mg of dex-HEMA and 5 μL of DMAEMA were added, and the mixture was stirred and sonicated, resulting in a 17% (w/w) dex-HEMA solution in water. For polystyrene encapsulation studies, 20 μL of the corresponding polystyrene suspension was also added to the monomer phase and the mixture was vortexed vigorously.

Microcapsule Fabrication. Monodisperse microgels were coated with alternating layers of Pt_{NP}'s and DAR. In total, three bilayers were deposited. The Pt_{NP} solution consisted of 0.5 mg/mL Pt_{NP}'s in the presence of 0.5 M NaCl in deionized water, and the DAR consisted of 1 mg/mL resin in the presence of 0.5 M NaCl in deionized water. Adsorption was carried out for 10 min under continuous shaking, and three washing/centrifugation steps were carried out to remove nonadsorbed species.

Microscopy. Confocal microscopy images were recorded with the transmission channel on a Nikon EZ-C1. Scanning electron microscopy (SEM) images were recorded with a Quanta 200 FEG FEI scanning electron microscope operated at an acceleration voltage of 5 kV. A drop of the particle or capsule suspension was deposited onto a silicon wafer and dried under a nitrogen stream followed by sputtering with gold. Transmission electron microscopy (TEM) images were recorded with a CM-200 FEG Philips transmission electron microscope operated at an acceleration voltage of 120 kV. A drop of Pt_{NP}'s suspension was deposited and dried onto a copper grid modified with amorphous carbon.

RESULTS AND DISCUSSION

The tubing-based microfluidic setup that is utilized in the present work is composed of simple tools that are readily available, i.e., syringe pumps, syringes, needles, tubing, and UV lamps (Figure 2A). It does not require any special reactor fabrication strategy such as soft lithography (43). The simplicity of the setup in combination with the capability of producing monodisperse beads makes it more attractive than other microfluidic systems. The original setup, reported by Quevedo et al. (44), was improved with some modifications. First, the tubing used in the present work is half of the diameter compared to the original setup, which allowed us to use 4 times less of the continuous phase to obtain the same material. Using flexible Tygon tubing instead of a Teflon one minimized leakage in the system. Moreover, simply bending the discrete phase needle 90° transformed the setup from a T-junction to a co-flow device (45), resulting in more reproducible bead formation.

An aqueous solution of dex-HEMA, DMAEMA (i.e., a cationic methacrylate at physiological conditions (46), providing the microgels with a positive surface charge) (47), and the photoinitiator Irgacure 2959 was pressurized by a syringe pump and fed in an inline fashion through a blunt needle into a continuous oil stream containing a nonionic surfactant (ABIL EM90). After the formation of monodisperse aqueous droplets in the oil stream, the tubing was directed into a UV chamber where radical polymerization of the methacrylate groups was initiated, resulting in the formation of solid monodisperse microgels. The oil stream was collected, and the microgels were transferred to water by several washing steps with acetone to remove the oil, finally allowing the microgels to be suspended in water. Figure 2B shows a stereomicroscopy image of the obtained microgels. The dense packing of the microgels in a hexagonal conformation illustrates their monodispersity. Image analysis was performed to determine the size distribution of the microgels, and the corresponding histogram is shown in Figure 2C, indicating a mean diameter of 290 μm and a narrow size distribution.

To evaluate whether Pt_{NP}'s and DAR can form multilayers by sequential deposition, their capability for multilayer buildup was first assessed on planar substrates and monitored by UV−vis spectroscopy. Figure 3A depicts wave scans recorded after the deposition of each single layer. Figure 3B shows the increase in absorbance at 380 nm, which is the absorption maximum of DAR. Because Pt_{NP}'s do not have a specific absorption maximum, the absorption increases stepwise with the deposition of each bilayer Pt_{NP}/DAR because of the strong absorbance of the DAR. The linear increase of the absorption as a function of the bilayer

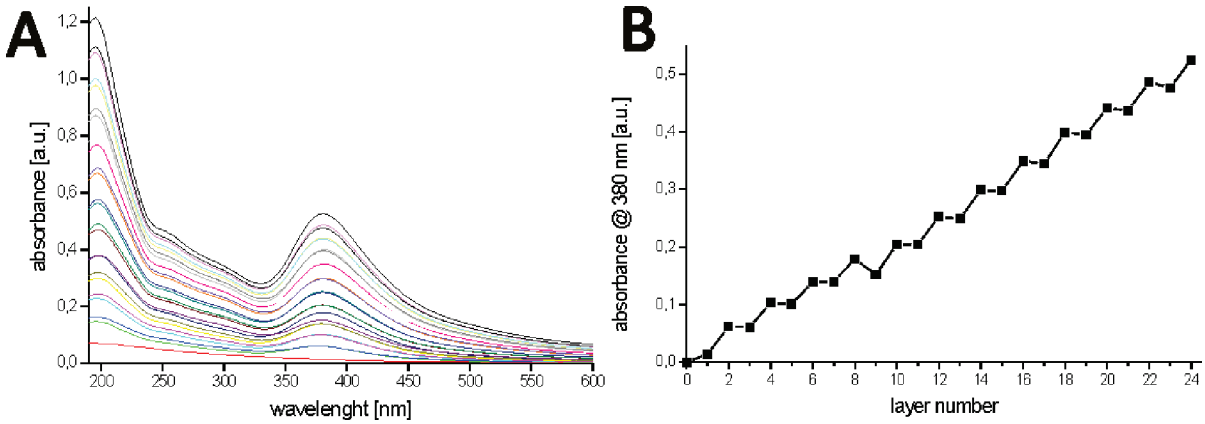

FIGURE 3. (A) UV−vis spectra of a quartz slide coated with 12 bilayers of Pt_{NP}/DAR. After deposition of each single layer, the UV−vis spectrum was recorded. (B) Increase in the absorbance at 380 nm as a function of the adsorption step.

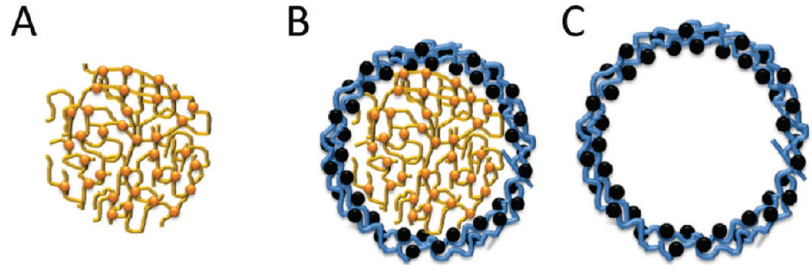

FIGURE 4. Schematic representation of the fabrication of hollow capsules. dex-HEMA microgels (A) are coated with a multilayer membrane consisting of anionic Pt_{NP}'s and cationic DAR (B). Hollow capsules (C) are obtained after dissolution of the dex-HEMA microgel template.

number clearly demonstrates the alternating adsorption of Pt_{NP}'s and DAR, forming a multilayer structure.

In a next step, the monodisperse microgels have been coated with three bilayers of Pt_{NP}'s and DAR. A schematic representation of the process is shown in Figure 4. The Pt_{NP}'s were synthesized according to Chen and Kimura by the reduction of hydrogen hexachloroplatinate with $NaBH_4$ (48). Capping with MSA functionalizes the Pt_{NP}'s surface with carboxylic acid moieties, providing them with a negative surface charge as confirmed by measurement of the electrophoretic mobility. Figure 1C shows a TEM image of the Pt_{NP}'s exhibiting size values roughly between 0.5 and 2 nm. The molecular structure of the cationic DAR and its light-induced cross-linking (which occurs even under ambient light conditions) (38) with the Pt_{NP}'s carboxylic acid moieties are shown in Figure 1D. Because the monodisperse microgels are positively charged as a result of incorporation of the cationic DMAEMA, the multilayer buildup was initiated with the anionic Pt_{NP}'s followed by the DAR. We have chosen a deposition of three bilayers because a number of bilayers between 2 and 4 are usually well suited for the fabrication of stable multilayer capsules (8, 36, 38, 49−52).

The $(Pt_{NP}/DAR)_3$-coated microgels were visualized with confocal microscopy (Figure 5B) and SEM (Figure 5D). Whereas uncoated microgels are observed as being optically very transparent (Figure 5A), the $(Pt_{NP}/DAR)_3$-coated microgels appear black and do not transmit light. This is due to the high density of the Pt_{NP}'s, which are kept together by the DAR. We have previously reported a similar observation using anionic gold nanoparticles in conjunction with cationic poly(allylamine hydrochloride) for the synthesis of 3-μm-sized hollow capsules templated on $CaCO_3$ microparticles (50, 51). SEM also reveals the presence of a coating surrounding the microgels. Whereas the surface of the uncoated microgels is smooth, the $(Pt_{NP}/DAR)_3$-coated microgels exhibit a "ball-in-a-bag" appearance due to the difference in drying kinetics between the microgels and the $(Pt_{NP}/DAR)_3$ coating. When the sizes of the microgels measured by optical and electron microscopy are compared, a 2-fold decrease in the diameter is observed by electron microscopy. This dramatic shrinkage is ascribed to the dehydratation step under vacuum prior to sputtering and SEM imaging.

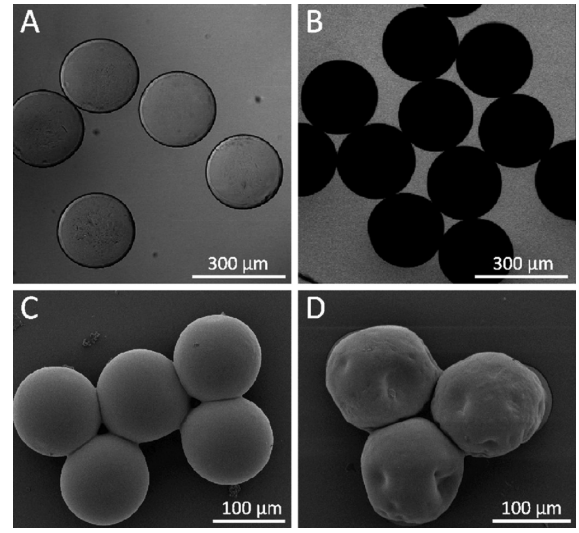

FIGURE 5. Confocal microscopy (transmission channel) of (A) uncoated and (B) $(Pt_{NP}/DAR)_3$-coated, monodisperse dex-HEMA microgels. (C and D) SEM images corresponding to parts A and B.

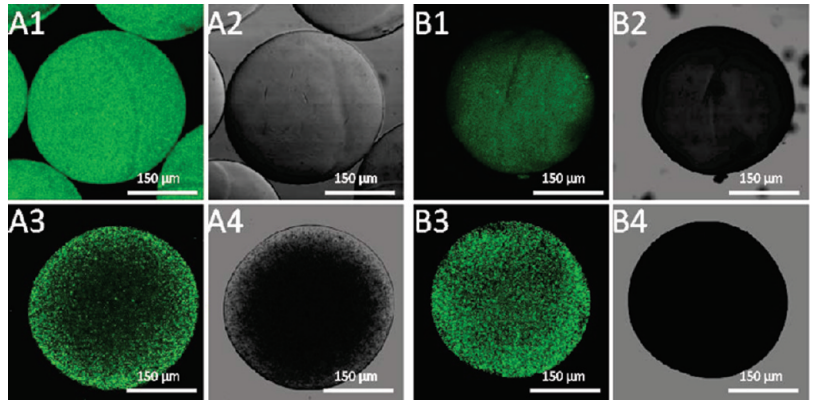

FIGURE 6. Confocal microscopy images of microgels encapsulating green fluorescent polystyrene beads (A) before and (B) after coating with $(Pt_{NP}/DAR)_3$. The upper row represents encapsulation of 100-nm-sized green fluorescent polystyrene beads, while the lower row represents encapsulation of 1-μm-sized polystyrene beads.

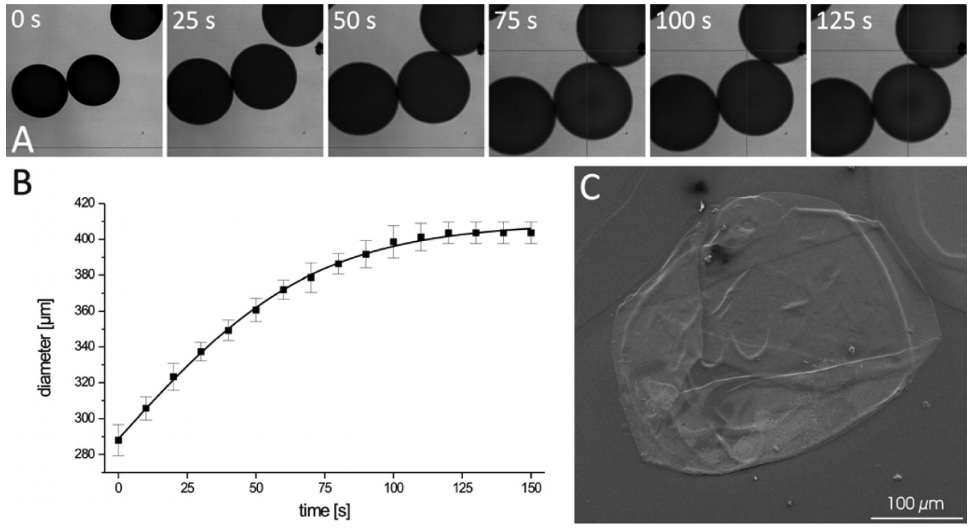

FIGURE 7. (A) Confocal microscopy (transmission channel) snapshots taken during the (NaOH-accelerated) degradation of $(Pt_{NP}/DAR)_3$-coated monodisperse dex-HEMA microgels resulting in hollow $(Pt_{NP}/DAR)_3$ capsules. (B) Evolution of the microgel diameter during the degradation process as measured by confocal software. (C) SEM image of a hollow $(Pt_{NP}/DAR)_3$ capsule.

To illustrate the possibility of encapsulation within the microgels, hydrophilic (carboxylated) green fluorescent polystyrene beads with diameters of 100 nm and 1 μm were added to the aqueous dex-HEMA feed stream prior to microfluidic emulsification in two different experiments. The rationale behind the encapsulation of these particles was to use them in future research for bead detection assays within the confined volume of a capsule, which could exhibit selective permeability for solutes of different sizes and would also allow easy transportation of the beads from one medium to another. Figure 6 shows the corresponding confocal microscopy images of the microgels obtained after UV polymerization. The fluorescent polystyrene particles are distributed throughout the volume of the microgels and can still be detected after coating with $(Pt_{NP}/DAR)_3$. Note that for transfer of the polystyrene-loaded microgels to the aqueous phase, ethanol was used as the intermediate solvent instead of acetone because this would have led to dissolution of the polystyrene particles.

Finally, in order to obtain hollow capsules, the microgel templates have to be dissolved. dex-HEMA hydrogels are degradable through hydrolysis of carbonate esters (53, 54), which connect the dextran backbone with the polymerized HEMA (29, 30). Therefore, the $(Pt_{NP}/DAR)_3$-coated microgels were suspended in a 1 M sodium hydroxide (NaOH) solution for 5 min and allowed to sediment, followed by removal of the supernatant and resuspension in distilled water. This process was repeated three times to ensure sufficient removal of residual NaOH. Note that centrifugation should be avoided to avoid capsule breakup. Figure 7 shows in detail the influence of microgel degradation on the capsule properties. Confocal microscopy (Figure 7A) shows that, upon the addition of NaOH, the microcapsules start to swell until equilibrium is reached after approximately 100 s of swelling, as illustrated by Figure 7B, which shows the gradual increase in the capsule diameter as a function of the degradation time until a plateau is reached. The physicochemical reason for this swelling is the swelling pressure, which increases upon degradation of the hydrogel network. As the number of cross-links decreases, the dextran chains have more flexibility within the network, allowing it to expand. Note that no relaxation of the capsule membrane was observed and the capsules retained their final diameter over prolonged times. The proof that hollow capsules are generated in this

way is given by SEM as a collapsed folded structure, which is typical for hollow polyelectrolyte capsules in the dried state.

CONCLUSIONS

Giant hollow polyelectrolyte capsules, with dimensions much larger than common (1−10-μm-sized) polyelectrolyte capsules, have been fabricated using degradable microgels as a sacrificial template. The microgels were synthesized by microfluidic emulsification in a co-flow geometry, allowing large monodisperse microgels to be produced. In order to help the capsule membrane withstand the swelling pressure of the degrading microgel, the membrane was reinforced using covalent linkages between a cationic polyelectrolyte and metal nanoparticles. This multilayer buildup between the polyelectrolyte and metal nanoparticles was demonstrated by the gradual increase of the UV absorption at 380 nm, proving the efficiency of the coating strategy. Microgels loaded with nano- or microsized fluorescent polystyrene particles have been prepared for encapsulation studies. Both types of polystyrene particles have been visualized, even after multilayer buildup. These microcapsules can find applications as microreactors (32−34) or delivery systems after remote opening of the microcapsules' shell by an external physical source such as laser light (55−59) or ultrasound (51, 60).

Acknowledgment. This research project has been supported by a Marie Curie Early Stage Research Training Fellowship of the European Community's Sixth Framework Programme under Contract No. 020643 (Sendichem project), which M.T.G. is grateful for. B.G.D.G. thanks the FWO for a postdoctoral fellowship. F.E.D.P. acknowledges the ESF program STIPOMAT and the Belgian Program on Interuniversity Attraction Poles initiated by the Belgian State, Prime Minister's office (Program P6/27) for financial support.

REFERENCES AND NOTES

(1) Bertrand, P.; Jonas, A.; Laschewsky, A.; Legras, R. *Macromol. Rapid Commun.* **2000**, *21*, 319–348.
(2) Decher, G. *Science* **1997**, *277*, 1232–1237.
(3) Lynn, D. M. *Soft Matter* **2006**, *2*, 269–273.
(4) Lynn, D. M. *Adv. Mater.* **2007**, *19*, 4118–4130.
(5) Angelatos, A. S.; Katagiri, K.; Caruso, F. *Soft Matter* **2006**, *2*, 18–23.
(6) Ariga, K.; Hill, J. P.; Ji, Q. M. *Phys. Chem. Chem. Phys.* **2007**, *9*, 2319–2340.
(7) Caruso, F.; Caruso, R. A.; Mohwald, H. *Science* **1998**, *282*, 1111–1114.
(8) De Geest, B. G.; Sanders, N. N.; Sukhorukov, G. B.; Demeester, J.; De Smedt, S. C. *Chem. Soc. Rev.* **2007**, *36*, 636–649.
(9) Peyratout, C. S.; Dahne, L. *Angew. Chem., Int. Ed.* **2004**, *43*, 3762–3783.
(10) Sukhorukov, G. B.; Donath, E.; Davis, S.; Lichtenfeld, H.; Caruso, F.; Popov, V. I.; Mohwald, H. *Polym. Adv. Technol.* **1998**, *9*, 759–767.
(11) Sukhorukov, G. B.; Donath, E.; Lichtenfeld, H.; Knippel, E.; Knippel, M.; Budde, A.; Mohwald, H. *Colloids Surf., A* **1998**, *137*, 253–266.
(12) Sukhorukov, G. B.; Mohwald, H. *Trends Biotechnol.* **2007**, *25*, 93–98.
(13) Sukhorukov, G. B.; Rogach, A. L.; Zebli, B.; Liedl, T.; Skirtach, A. G.; Kohler, K.; Antipov, A. A.; Gaponik, N.; Susha, A. S.; Winterhalter, M.; Parak, W. J. *Small* **2005**, *1*, 194–200.
(14) Sukhorukov, G. B.; Volodkin, D. V.; Gunther, A. M.; Petrov, A. I.; Shenoy, D. B.; Mohwald, H. *J. Mater. Chem.* **2004**, *14*, 2073–2081.
(15) Zhu, H. G.; Srivastava, R.; McShane, M. J. *Biomacromolecules* **2005**, *6*, 2221–2228.
(16) De Geest, B. G.; Dejugnat, C.; Prevot, M.; Sukhorukov, G. B.; Demeester, J.; De Smedt, S. C. *Adv. Funct. Mater.* **2007**, *17*, 531–537.
(17) Pommersheim, R.; Schrezenmeir, J.; Vogt, W. *Macromol. Chem. Phys.* **1994**, *195*, 1557–1567.
(18) Wang, Y.; Angelatos, A. S.; Caruso, F. *Chem. Mater.* **2008**, *20*, 848–858.
(19) Sivakumar, S.; Gupta, J. K.; Abbott, N. L.; Caruso, F. *Chem. Mater.* **2008**, *20*, 2063–2065.
(20) Gupta, J. K.; Tjipto, E.; Zelikin, A. N.; Caruso, F.; Abbott, N. L. *Langmuir* **2008**, *24*, 5534–5542.
(21) Tjipto, E.; Cadwell, K. D.; Quinn, J. F.; Johnston, A. P. R.; Abbott, N. L.; Caruso, F. *Nano Lett.* **2006**, *6*, 2243–2248.
(22) Thorsen, T.; Roberts, R. W.; Arnold, F. H.; Quake, S. R. *Phys. Rev. Lett.* **2001**, *86*, 4163–4166.
(23) Xu, S. Q.; Nie, Z. H.; Seo, M.; Lewis, P.; Kumacheva, E.; Stone, H. A.; Garstecki, P.; Weibel, D. B.; Gitlin, I.; Whitesides, G. M. *Angew. Chem., Int. Ed.* **2005**, *44*, 724–728.
(24) Kim, J. W.; Utada, A. S.; Fernandez-Nieves, A.; Hu, Z. B.; Weitz, D. A. *Angew. Chem., Int. Ed.* **2007**, *46*, 1819–1822.
(25) Nie, Z. H.; Li, W.; Seo, M.; Xu, S. Q.; Kumacheva, E. *J. Am. Chem. Soc.* **2006**, *128*, 9408–9412.
(26) Nie, Z. H.; Xu, S. Q.; Seo, M.; Lewis, P. C.; Kumacheva, E. *J. Am. Chem. Soc.* **2005**, *127*, 8058–8063.
(27) Zhang, H.; Tumarkin, E.; Peerani, R.; Nie, Z.; Sullan, R. M. A.; Walker, G. C.; Kumacheva, E. *J. Am. Chem. Soc.* **2006**, *128*, 12205–12210.
(28) De Geest, B. G.; Urbanski, J. P.; Thorsen, T.; Demeester, J.; De Smedt, S. C. *Langmuir* **2005**, *21*, 10275–10279.
(29) van Dijk Wolthuis, W. N. E.; Hoogeboom, J. A. M.; van Steenbergen, M. J.; Tsang, S. K. Y.; Hennink, W. E. *Macromolecules* **1997**, *30*, 4639–4645.
(30) van Dijk Wolthuis, W. N. E.; Tsang, S. K. Y.; Kettenes van den Bosch, J. J.; Hennink, W. E. *Polymer* **1997**, *38*, 6235–6242.
(31) Priest, C.; Quinn, A.; Postma, A.; Zelikin, A. N.; Ralston, J.; Caruso, F. *Lab Chip* **2008**, *8*, 2182–2187.
(32) Wang, B.; Zhao, Q. H.; Wang, F.; Gao, C. Y. *Angew. Chem., Int. Ed.* **2006**, *45*, 1560–1563.
(33) Choi, W. S.; Park, J. H.; Koo, H. Y.; Kim, J. Y.; Cho, B. K.; Kim, D. Y. *Angew. Chem., Int. Ed.* **2005**, *44*, 1096–1101.
(34) Shchukin, D. G.; Sukhorukov, G. B. *Adv. Mater.* **2004**, *16*, 671–682.
(35) De Geest, B. G.; Dejugnat, C.; Sukhorukov, G. B.; Braeckmans, K.; De Smedt, S. C.; Demeester, J. *Adv. Mater.* **2005**, *17*, 2357–2361.
(36) De Geest, B. G.; De Koker, S.; Immesoete, K.; Demeester, J.; De Smedt, S. C.; Hennink, W. E. *Adv. Mater.* **2008**, *20*, 3687–3691.
(37) De Geest, B. G.; Dejugnat, C.; Verhoeven, E.; Sukhorukov, G. B.; Jonas, A. M.; Plain, J.; Demeester, J.; De Smedt, S. C. *J. Controlled Release* **2006**, *116*, 159–169.
(38) De Geest, B. G.; McShane, M. J.; Demeester, J.; De Smedt, S. C.; Hennink, W. E. *J. Am. Chem. Soc.* **2008**, *130*, 14480–14482.
(39) De Geest, B. G.; Stubbe, B. G.; Jonas, A. M.; Van Thienen, T.; Hinrichs, W. L. J.; Demeester, J.; De Smedt, S. C. *Biomacromolecules* **2006**, *7*, 373–379.
(40) Markutsya, S.; Jiang, C. Y.; Pikus, Y.; Tsukruk, V. V. *Adv. Funct. Mater.* **2005**, *15*, 771–780.
(41) Kotov, N. A.; Magonov, S.; Tropsha, E. *Chem. Mater.* **1998**, *10*, 886–895.
(42) Zhu, H. G.; McShane, M. J. *Langmuir* **2005**, *21*, 424–430.
(43) Becker, H.; Gärtner, C. *Anal. Bioanal. Chem.* **2008**, *390*, 89–111.
(44) Quevedo, E.; Steinbacher, J.; McQuade, D. T. *J. Am. Chem. Soc.* **2005**, *127*, 10498–10499.
(45) Utada, A. S.; Chu, L.-Y.; Fernandez-Nieves, A.; Link, D. R.; Holtze, C.; Weitz, D. A. *MRS Bull.* **2007**, *32*, 702–708.
(46) van de Wetering, P.; Zuidam, N. J.; van Steenbergen, M. J.; van der Houwen, O.; Underberg, W. J. M.; Hennink, W. E. *Macromolecules* **1998**, *31*, 8063–8068.
(47) Van Tomme, S. R.; van Steenbergen, M. J.; De Smedt, S. C.; van Nostrum, C. F.; Hennink, W. E. *Biomaterials* **2005**, *26*, 2129–2135.
(48) Chen, S. H.; Kimura, K. *J. Phys. Chem. B* **2001**, *105*, 5397–5403.
(49) De Geest, B. G.; De Koker, S.; Sukhorukov, G. B.; Kreft, O.; Parak, W. J.; Skirtach, A. G.; Demeester, J.; De Smedt, S. C.; Hennink, W. E. *Soft Matter* **2009**, *5*, 282–291.

(50) De Geest, B. G.; Skirtach, A. G.; De Beer, T. R. M.; Sukhorukov, G. B.; Bracke, L.; Baeyens, W. R. G.; Demeester, J.; De Smedt, S. C. *Macromol. Rapid Commun.* **2007**, *28*, 88–95.
(51) De Geest, B. G.; Skirtach, A. G.; Mamedov, A. A.; Antipov, A. A.; Kotov, N. A.; De Smedt, S. C.; Sukhorukov, G. B. *Small* **2007**, *3*, 804–808.
(52) De Geest, B. G.; Vandenbroucke, R. E.; Guenther, A. M.; Sukhorukov, G. B.; Hennink, W. E.; Sanders, N. N.; Demeester, J.; De Smedt, S. C. *Adv. Mater.* **2006**, *18*, 1005.
(53) De Geest, B. G.; Van Camp, W.; Du Prez, F. E.; De Smedt, S. C.; Demeester, J.; Hennink, W. E. *Chem. Commun.* **2008**, 190–192.
(54) De Geest, B. G.; Van Camp, W.; Du Prez, F. E.; De Smedt, S. C.; Demeester, J.; Hennink, W. E. *Macromol. Rapid Commun.* **2008**, *29*, 1111–1118.
(55) Radt, B.; Smith, T. A.; Caruso, F. *Adv. Mater.* **2004**, *16*, 2184.
(56) Skirtach, A. G.; Antipov, A. A.; Shchukin, D. G.; Sukhorukov, G. B. *Langmuir* **2004**, *20*, 6988–6992.
(57) Skirtach, A. G.; Dejugnat, C.; Braun, D.; Susha, A. S.; Rogach, A. L.; Parak, W. J.; Mohwald, H.; Sukhorukov, G. B. *Nano Lett.* **2005**, *5*, 1371–1377.
(58) Skirtach, A. G.; Javier, A. M.; Kreft, O.; Kohler, K.; Alberola, A. P.; Mohwald, H.; Parak, W. J.; Sukhorukov, G. B. *Angew. Chem., Int. Ed.* **2006**, *45*, 4612–4617.
(59) Skirtach, A. G.; Karageorgiev, P.; De Geest, B. G.; Pazos-Perez, N.; Braun, D.; Sukhorukov, G. B. *Adv. Mater.* **2008**, *20*, 506.
(60) Skirtach, A. G.; De Geest, B. G.; Mamedov, A.; Antipov, A. A.; Kotov, N. A.; Sukhorukov, G. B. *J. Mater. Chem.* **2007**, *17*, 1050–1054.

AM900055B